Article

Not peer-reviewed version

A New Sustainable PPT Coating Based on Recycled PET to Improve the Durability of Hydraulic Concrete

A. Borquez-Mendivil , C.P. Barrios-Durstewitz , R.E. Núñez-Jaquez , A. Hurtado-Macías , J.E. Leal-Pérez , J. Flores-Valenzuela , B.A. García-Grajeda , F.G. Cabrera-Covarrubias , J.M. Mendivil-Escalante * , J.L. Almaral-Sánchez *

Posted Date: 9 April 2024

doi: 10.20944/preprints202404.0661.v1

Keywords: Sustainability; PPT coating; recycled PET; durability; hydraulic concrete

Article

A New Sustainable PPT Coating Based on Recycled PET to Improve the Durability of Hydraulic Concrete

A. Bórquez-Mendivil [1], C.P. Barrios-Durstewitz [1], R.E. Núñez-Jáquez [1], A. Hurtado-Macías [2], J.E. Leal-Pérez [1], J. Flores-Valenzuela [1], B.A. García-Grajeda [1], F.G. Cabrera-Covarrubias [1], J.M. Mendivil-Escalante [1,*] and J.L. Almaral-Sánchez [1,*]

[1] Universidad Autónoma de Sinaloa. Gral. Ángel Flores S/N, Fracc. Las Fuentes, Los Mochis, Sin., C.P. 81223, México; adrian.borquez.fim@uas.edu.mx (A.B-M); durstewitz@uas.edu.mx (C.P. B-D); ronunez@uas.edu.mx (R.E. N-J); Eduardo.leal@uas.edu.mx (J.E. L-P); jflores@uas.edu.mx (J. F-V); blanca.garcia@uas.edu.mx (B.A. G-G); guadalupe.cabrera@uas.edu.mx (F.G. C-C); miguel.mendivil@uas.edu.mx, (J.M. M-E); jalmaral@uas.edu.mx (J.L. A-S)

[2] Centro de Investigación en Materiales Avanzados, S. C., Miguel de Cervantes #120, Complejo Industrial Chihuahua, Chihuahua, Chihuahua, 31136, México; abel.hurtado@cimav.edu.mx

* Correspondence: jalmaral@uas.edu.mx, J.L. A-S; miguel.mendivil@uas.edu.mx, (J.M. M-E)

Abstract: A new sustainable polypropylene terephthalate (PPT) coating was synthesized from recycled polyethylene terephthalate (PET) and applied on hydraulic concrete substrate to improve its durability. First step, PET bottles wastes were grinded and depolymerized by glycolysis using propylene glycol (PG), in a Vessel-type reactor (20–180 °C) to synthesize bis(2-hydroxypropyl)-terephthalate (BHPT), which was applied as coating to one-three layers on hydraulic concrete substrate, by brushing technique and polymerized (150 °C for 15 h) to obtain PPT. PET, BHPT and PPT were characterized by FT-IR, PET and PPT by TGA, and the PPT coatings by SEM (thickness), by ASTM-D3359-17 (adhesion) and by water contact angle (wettability). The durability of hydraulic concrete coated with PPT was studied by resist chloride ion penetration (ASTM-C1202-17), carbonation depth at 28 days (RILEM-CPC-18), and absorption water ratio (ASTM-C1585-20). The results demonstrated that the BHPT and PPT were synthetized (FT-IR), PPT had a similar thermal behaviour to PET (TGA); the PPT coatings had good adhesion to the substrate, with thicknesses of micrometric units; hydrophilic (similar to PET coatings), and the durability of hydraulic concrete coated with PPT (2-3 layers) improved (migration of chloride ions decreased, carbonation depth was negligible, and the absorption water ratio decreased).

Keywords: sustainability; PPT coating; recycled PET; durability; hydraulic concrete

1. Introduction

In recent decades, industrial growth and the expansion of consumables production have led to an exponential increase in the generation of polymeric waste, including polyethylene terephthalate (PET) [1]. PET is a thermoplastic polymer widely used in the production of beverage and food containers, which has reached a critical point in its life cycle, a situation that makes it an environmental and economic challenge due to its inadequate final disposal and permanence in environment [2]. Faced with the urgent need to address the pollution generated by polymeric waste and the transition to more sustainable practices, PET recycling has become a fundamental response [3]. In 2019, an annual production of 30.5 million tons of PET was reported in the world and by 2024 it is expected to be around 35.3 million tons [4], corresponding to the generation of PET bottles, which would subsequently be wasted, that has generated the interest in exploring alternatives for recycling and converting them into new materials with added value [5].

PET recycling can be carried out in different recycling phases: primary, secondary, tertiary, and quaternary. Mechanical and chemical methods have been commonly reported, which comprise the secondary and tertiary phases of their recycling, respectively [6]. Mechanical recycling consists of the

 doi:10.20944/preprints202404.0661.v1

collection, sorting, and grinding of PET bottles, resulting in the production of flakes, fibers, or powders [7]. On the other hand, chemical recycling, particularly by glycolysis, causes the controlled degradation of PET into monomers or oligomers of lower molecular weight, known as glycolyzed products [8]. These have been used for the synthesis of a wide range of materials such as resins, coatings, and adhesives [9–11]. Powders obtained from post-consumer bottles PET were applied on mild steel substrates as anti-corrosive coatings [12]. However, it is important to consider that the PET bottle recycling process, especially mechanical recycling, is the most important generator of large quantities of microplastics, because during the crushing and screening of PET bottles, to produce the sizes of this material and continue with the chemical process, very small sized particles (microplastics) are also produced, which are collected in the waste water of said process and whose treatment produces waste sludge, in which said microplastics are trapped and at the time of their final disposal, they are transferred to the environment (through the sewage network, rivers, oceans or soil), which becomes a challenge that should not be ignored [13]. Furthermore, humans are exposed to the ingestion of microplastics, which, if it becomes chronic, may represent a risk that would affect their immune microenvironment [14].

In the construction industry, innovation has been fundamental to the development of sustainable and long-lasting solutions. Products derived from PET recycling have shown potential to improve the properties and useful life of building materials, for example: it has been applied as reinforcing fibers for cementitious materials [15–17], incorporated in the manufacture of asphalt mixtures [18], and soil stabilizer [19]. Hydraulic concrete is the most used material in the construction industry and maintaining its durability is very important to ensure that it meets the life service for which it was designed [20]. This can be achieved with proper mix design [21] or application of coatings. Coating of acrylic [22], epoxy resin [22-23], cementitious coating modified with nanoSiO_2 and hybrid nanoSiO_2 [23], silane cream (alkylalkoxysilane) and silane gel (triethoxysilane) [24], acrylate terpolymer based [25], magnesium fluorosilicate, waterglass, sodium fluorosilicate [26], interior and exterior paints [27], calcium silicate, and acrylic-silicon [28], were applied on concrete and studied for carbonatation. Coating of epoxy resin modified with graphene oxide [29], nano-silica, silane/nanoclay [30], chlorinated rubber, polyurethane [31], and alkiltrialkoxisilane [32] were used on concrete for improve its resistance and permeability to chloride ion. Coating of epoxy resin modified with graphene oxide [29], silane-based water repellent agent as alkylalkoxy silane [33], isobutyltriethoxysilane [34], fluoroalkyl silane modified with rice husk ash [35], and silane/siloxane [32] were employed on concrete and studied its performance in water absorption. Hydraulic concrete coated with polyurethane has presented a low risk of corrosion by obtaining its electrical resistivity [36].

After an exhaustive literature review, the synthesis and application of PPT coating based on recycled PET to improve the durability of hydraulic concrete was not found. The success of our research was to develop a new sustainable polypropylene terephthalate (PPT) coating from recycled polyethylene terephthalate (PET), synthesized by a simple method and applied by brush, which improved the durability of hydraulic concrete. BHPT and PPT were characterized by FT-IR, PPT and PET by TGA. The coatings were characterized by SEM, contact angle, adhesion, carbonation depth, permeability of chloride ions and water absorption.

2. Materials and Methods

2.1. Materials

Post-consumer PET soft drink bottles were mechanically recycled by grinding to reduce them to flakes of 1/2 in and washed with a 10% NaOH solution. Propylene glycol (PG), ≥99%, zinc acetate (ZnA), tetrahydrofuran (THF), ethanol, and distilled water, were used for the depolymerization of PET and obtaining BHPT. The reagents were Sigma-Aldrich brand and supplied by Merck-Mexico. Ordinary Portland cement type III CEMEX brand, CPC, according with ASTM C150, and natural aggregates (gravel and sand) were purchased from CONSTRURAMA, S.A. of C.V. and water was supplied by the local drinking water network.

 doi:10.20944/preprints202404.0661.v1

2.2. Synthesis of the bis(2-hidroxyproyl) Terephthalate (BHPT) Monomers

The chemical recycling process for PET bottles implied their depolymerization with propylene glycol to obtain the BHPT monomers. The procedure was carried out in the following stages: The PET flakes were deposited in a Syrris Vessel-type reactor at room temperature. PG was added at a rate of 100% by weight of PET, and zinc acetate was added as a catalyst at a rate of 0.5% by weight of PET. After that, these reagents were mixed with mechanical stirring at room temperature for 15 min. Next the subsequent temperature increased in steps rate of 5 °C/min from 20 °C to 180 °C for 3 h. Then it was kept at rest until reached room temperature for later use. As a result of the process, the product is likely to be BHPT, and excess unreacted PG and EG formed as a by-product.

2.3. Purification Process of BHPT

The BHPT monomers obtained were subjected to a purification process to eliminate excess unreacted PG and EG formed as a by-product during their synthesis. EtOH and THF, 100% and 20% by volume of BHPT, respectively, were stirred in a beaker for 15 min. Then, the BHPT monomers were added to the mixture and stirred for 30 min at room temperature. Next, three washes were performed with distilled water, each with a volume equivalent to 30% by volume of BHPT for 15 min. The solution was vacuum filtered in a Buchner funnel, after that, it was dried in an oven with air circulation at 60 °C for 24 hours and kept at rest until reaching room temperature for use in later stages.

2.4. Synthesis of Polypropylene Terephthalate (PPT)

The synthesis of PPT was carried out in the following steps: 1) The purified BHPT monomer, at room temperature, was poured into circular molds of 2.5 cm in diameter and 1.5 cm in height, to prepare bulk composites, after that, 2) The molds with the BHPT were placed in an oven with air circulation, at 150 °C for 15 h, for polymerization, and thus synthesizing the PPT.

2.5. Elaboration of Cementitious Concrete Mixes

A low-strength concrete mixture (150 kg/cm^2) with a water/cement ratio of 0.8 was elaborated, with the objective of studying the effect of the polypropylene terephthalate (PPT) coating on porous concrete. Table 1 shows the dosage used, which was calculated following the method established by the ACI 211.1-22 method [37]. The preparation of the mixture was carried out as described in the ASTM C31/C31M-22 standard. This mixture was poured into cylindrical metal molds 10 cm in diameter and 20 cm high. Once the mixture had set, it was cured in water for 28 days. After this period, it was cut into 5 cm thick slices and stored for later application of the coating.

Table 1. Dosage of the mixture for 1 m^3 of hydraulic concrete.

Material	Dosage (Kg/m^3)
Cement	256.25
Water	205.00
Coarse aggregate	1024.00
Fine aggregate	608.40

2.6. Elaboration of PPT Coatings Hydraulic Concrete by Brush

The hydraulic concrete specimens were previously prepared to ensure adequate application and adhesion of the PPT coating with its surface, which was free of contaminants, laitance, loose concrete, and dust, in accordance with the SSPC-SP-13 /NACE No. 6 standard. Subsequently, the BHPT was applied to the surface of the concrete by brush in three layers, at room temperature, and for each coated layer, the specimens were placed in an oven with air circulation under the polymerization conditions described in 2.4, to subsequently achieve PPT coating formation. The nomenclature for

 doi:10.20944/preprints202404.0661.v1

the studied specimens was declared as follows: REF for uncoated reference concrete, CB1, CB2, and CB3 for concrete coated with 1, 2 and 3 layers, respectively.

2.6. Characterization

2.6.1. FT-IR

The PET, PPT, and BHPT samples were analyzed by the FT-IR technique to identify their characteristic bonds using a Nicolet iS50 spectrometer with transmission configuration. The three types of materials had different treatments for FT-IR analysis, PET was reduced to powder; PPT was condensed (in oven at 150°C for 15 h) and reduced to powder; BHPT analyzed in liquid state. The samples were placed on a diamond surface and the spectroscopic measurements were carried out within the wavelength range of 4000 to 400 cm^{-1} with the help of attenuated total reflectance fixtures.

2.6.2. TGA

The thermal stability of PET, and PPT was evaluated by thermogravimetric analysis (TGA). This analysis was performed using the TA Instrument SDT-Q600 simultaneous equipment under an oxygen atmosphere, with a heating rate set at 10 °C per minute, within a temperature range spanning 0 to 700 °C.

2.6.3. Physical Properties of Coatings

Thickness of coating was examined with a scanning electron microscope (SEM); this analysis was performed with the JEOL SEM model JSM5800LV microscope. The samples consisted of small representative fragment of coated concrete with three layers of PPT, without prior preparation to avoid modification or degradation of the organic coating.

The adhesion of the coatings was evaluated using Cross Section Test Method B of ASTM D3359-17 [38], in which a grid is made on the coated substrate with a line spacing of 2 mm and then an adhesive tape is placed over the grid by pressure and after a certain time it is removed. Adhesion strength grades are based on the percentage of coating removed after testing, with levels ranging from 0B (very poor adhesion) to 5B (very good adhesion).

The wettability of coatings to determine their hydrophilicity or hydrophobicity was determined using an FTA 200 contact angle analyzer (First Ten Armstrong in Ports-mouth, VA, USA), using samples of the coated substrates (3 cm x 9 cm), which were placed horizontally and drops of 10 µl of distilled water were applied six times to the surface of the coating, and the resulting data were analyzed to calculate the mean value and standard deviation, which were then reported.

2.6.4. Durability Tests

The water absorption rate was evaluated according to ASTM C1585-20 [39], in which the evaluated samples consisted of slices 10 cm in diameter and 5 cm high, in which only one side is exposed to a sheet of water of 2 $\pm$ 1 mm at times of 1, 5, 10, 20, 30 min and 1, 2, 3, 4, 5, and 6 h. Afterwards, the absorption in mm produced by capillarity is calculated by mass difference.

The resist chloride ion penetration was carried out according to ASTM C1202-19 [40] standard, in which the samples consist in slices 10 cm in diameter and 5 cm high with only one face covered with coating. The samples were placed between two cells, one was acted as cathode electrode filled with NaOH aqueous solution (0.3 N) in which the uncovered face was exposed, and the other one as anode electrode filled with NaCl aqueous solution (3 %) in which the covered face was exposed. The chloride ion permeability classification of the specimens was obtained in accordance with the same standard.

The carbonation depth was carried out according to the RILEM CPC-18 standard [41], after 7, 14, and 28 days of exposure to CO_2, in an accelerated carbonation chamber with the following conditions: temperature of 25 $\pm$ 3 °C, average relative humidity of 60 $\pm$ 5% and average CO_2 concentration of 5%. The specimens were sprayed with a diluted phenolphthalein solution (1% in

 doi:10.20944/preprints202404.0661.v1

ethyl alcohol), this is an indicator that reacts with non-carbonated areas changing its color to purple. The carbonation depth of the samples was obtained with the average of 9 measurements made with a digital Vernier.

3. Results and Discussion

3.1. Proposed Schematic Drawing of the Synthesis of PPT from PET Recycling

The Figure 1 shows the proposed schematic drawing of the synthesis of polypropylene terephthalate (PPT) from the chemical recycling of PET wastes. PPT is synthesized in two stages: First, PET is depolymerized by glycolysis using PG as solvent with a catalyst to form the BHPT monomers, excess unreacted PG and EG formed as a by-product. After that, the BHPT monomers are purified to remove excess PG and EG [8]. In a second stage, the BHPT monomers are condensed in temperature conditions to form PPT [42-43].

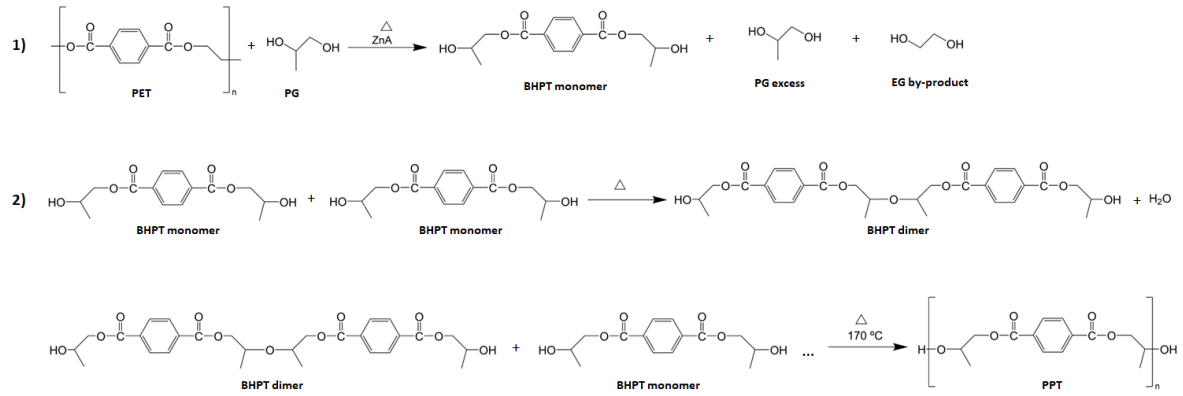

Figure 1. Proposed schematic drawing of the synthesis of PPT from PET recycling.

3.2. FT-IR

The Figure 2 presents the FT-IR spectra of the PET, BHPT and PPT samples. a) shows the entire range of wave numbers studied, b)–d) are amplified regions of study. The spectra, previously normalized to their maximum transmittance value, were arbitrarily shifted on the same transmittance axis. In a), the following bands were observed: For PET, C=O stretching bands (carbonyl group) around 1720-1750 cm^{-1}, asymmetric and symmetric C-H stretching bands (CH_2-group) around 2950-2960 and 2880-2900 cm^{-1}, and C=C stretching bands in the aromatic ring around 1600-1620 cm^{-1} were identified [44]. For BHPT, the same characteristic bands as in PET were observed, which confirms the persistence of the basic structure of PET ; (1720-1750 cm^{-1} for C=O stretching, 2950-2960 and 2880-2900 cm^{-1} for CH_2 and CH groups, respectively, and 1600-1620 cm^{-1} for C=C stretching bands). Furthermore, a new broad band was identified between 3200-3600 cm^{-1}, corresponding to the stretching of the hydroxyl group (OH) [45], and a band around 2980 cm^{-1}, attributed to the presence of CH_3 groups, which confirm the obtaining of BHPT by transesterification between PET and propylene glycol [46].The spectrum of PPT is visually very similar to that of PET with some differences related to the presence of propyl groups in its molecule produced during the polycondensation of BHPT. These differences can be observed in detail in the magnifications presented in b), c), and d), which are described below. In b) is shown the magnification of the C-H stretching region (2950-2960 and 2880-2900 cm^{-1}), moreover, were observed a band at 2981 cm^{-1} in the PPT sepctrum that is absent in PET spectrum, this difference is atribuited at the presence of propylene groups in PPT molecule. In Figure c), in the PPT spectrum we can observe the appearance of two bands at 1452 and 1379 cm^{-1} corresponding to bendings vibrations of CH_3 groups, signals absent in the PET spectrum. In Figure d), the different bands between the PET and PPT spectra are indicated, in the latter the bands at 987, 937, 920 and 811 cm^{-1} are indicated, which are characteristics of polypropylene [47-48].

 doi:10.20944/preprints202404.0661.v1

The differences between the PET and PPT spectra showed that PPT was synthesized because PET was synthesized from ethylene glycol while PPT from PET wastes by transterification (glycolysis) from propylene glycol.

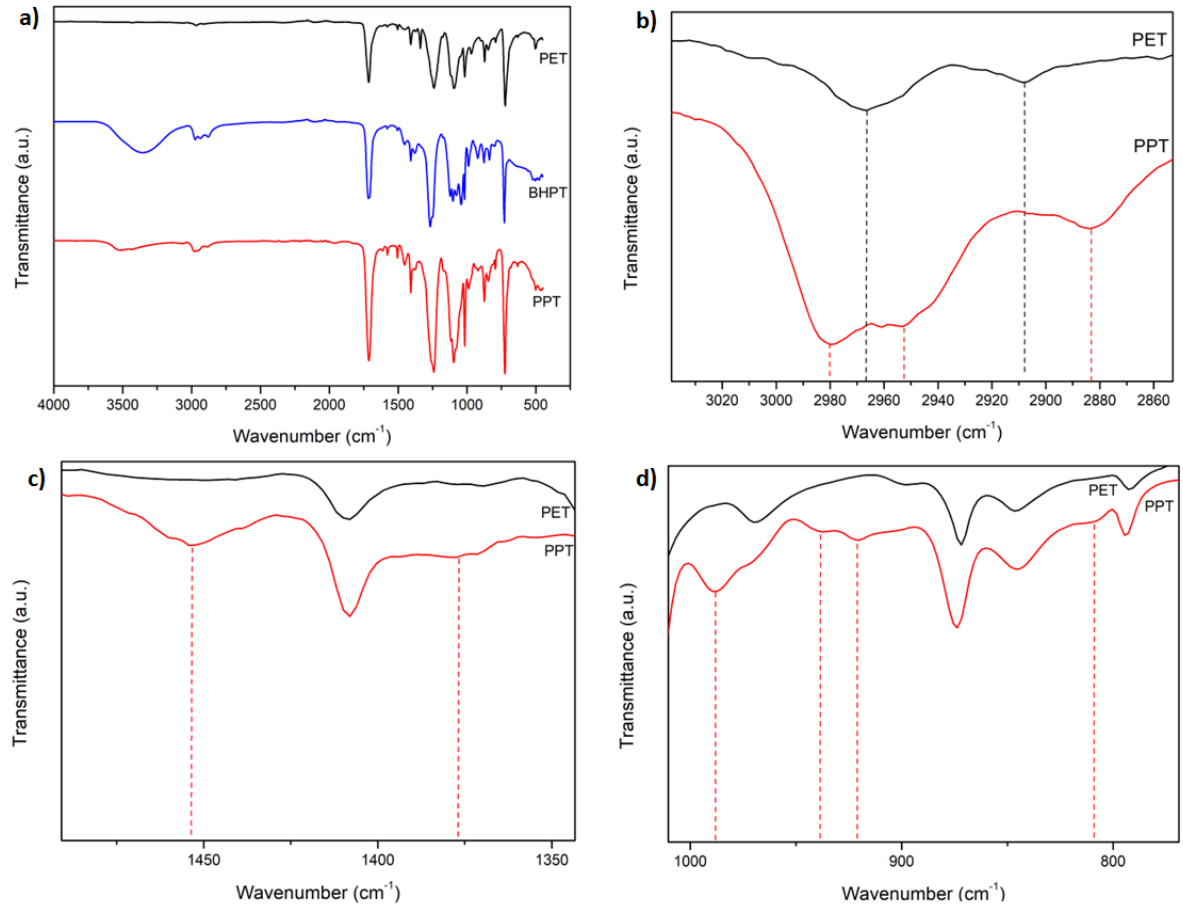

Figure 2. FT-IR spectrum of: a) PET, BHPT, and PPT at wavenumber region 4000-400 cm^{-1}, b) PET and PPT at wavenumber region 3040-2850 cm^{-1}, c) PET and PPT at wavenumber region 1500-1350 cm^{-1}, and d) PET and PPT at wavenumber region 1000-800 cm^{-1}.

3.3. TGA

Figure 3 shows the TGA of PET and PPT. For PET, a two-stage degradation was observed, the first mass loss was of 93% (361-450 °C) related to the random cleavage of the ester bond resulting in the formation of oligomers, the second degradation observed was of 7% (450-518 °C) attributed at carbonyl group decomposition [49-54]. For the PPT, a first mass loss was of 2.5% (30-210 °C) related to residual -OH groups that did not participate during the condensation of the BHPT, it continues with a second mass loss of 10.5 % (210-312 °C), attributed to the decomposition of groups CH, and a third mass loss of 80% (312-445 °C), which may correspond to the presence of a carbon-carbon bond that promotes the random cleavage of the ester bond mechanism with increasing temperature [49]. The results of TGA show that the main degradation of the PPT sample started at temperature near (312 °C) to that of PET (348 °C). That indicates that PPT has a thermal behaviour similar than the PET.

 doi:10.20944/preprints202404.0661.v1

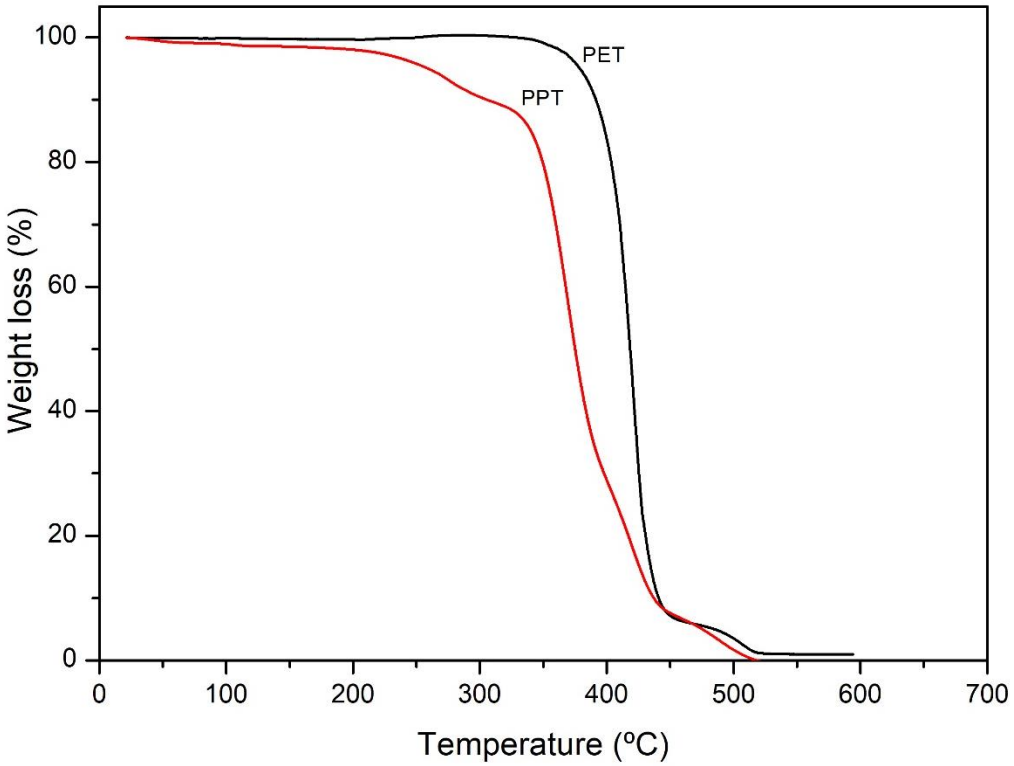

Figure 3. Thermogram of PET and PPT samples.

3.4. Physical Properties of PPT and Coatings

3.4.1. Appearance

Figure 4 shows the appearance of the PPT obtained through the polymerization of BHPT, a reddish-brown solid bulk sample capable of being demolded is observed.

Figure 4. Appearance of PPT bulk sample.

Figure 5 shows the photographs of the reference concrete specimens (REF) and coated with 1 layer (BC1), 2 layers (BC2) and 3 layers (BC3) of PPT. It can be seen that in BC1, the shade of the mortar paste does not present a visible change, so it is similar to that of REF. In BC2, most of the section became darker in REF. While in BC3, the entire section is darker and more uniform in color than BC2. At first glance, it can be concluded that in BC2 and BC3 the coating is perceptible and that in BC3 it was applied to the entire surface.

 doi:10.20944/preprints202404.0661.v1

Figure 5. Appearance of the uncoated concrete specimens (REF) and coated with PPT (BC1, BC2 and BC3).

3.4.2. Thickness

Figure 6 shows the SEM micrograph of the cross section of coated concrete with three layers of PPT, with several thickness measurements, which were very similar between them. The average thickness of PPT coating was 2.50 μm.

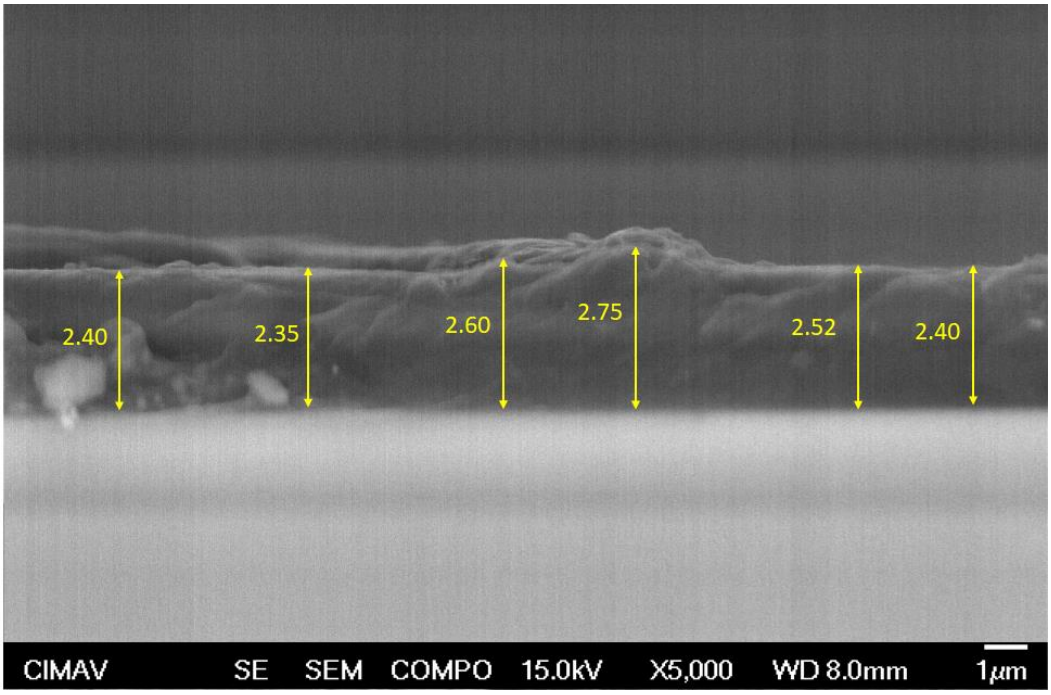

Figure 6. SEM micrograph of the cross section of PPT coating with several thickness.

3.4.3. Adhesion.

Figure 7 shows shows three photographs of samples BC1, BC2 and BC3, which were tested using ASTM D3359-17 (cross section test method). It can see that there was no detachment of material from the interior of the squares formed when making the cuts (area removed from 0%). Therefore, the samples presented very good adhesion with the concrete and were classified as 5B, according to the cited standard. These results are similar to those reported for coatings elaborated with resins synthesized from glycolized PET products on glass and metal substrates [9, 11].

 doi:10.20944/preprints202404.0661.v1

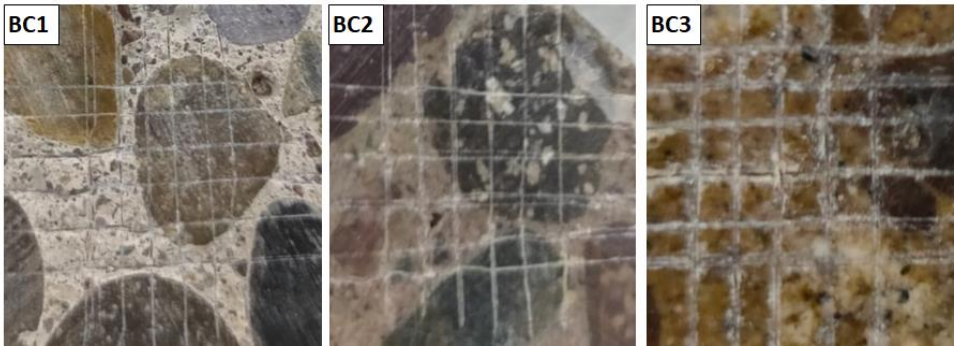

Figure 7. Photographs of the samples (BC1, BC2, and BC3) tested by cross-cut method adhesion (ASTM D3359-17).

3.4.4. Wettability Capacity (Water Contact Angle, WCA)

The average WCA of PPT coating was 72.90° ± 1.51, this measurement indicates a hydrophilic behavior, similar to that reported for PET sheets (78°) [55], PET films (60°), PET/fluorinated oligomeric polyester composite coatings (70-88°) [56], and PET coatings (68-78°) [57].

3.5. Durability Properties of Concrete

3.5.1. Rate of Absorption of Water (ASTM C1585-20)

Figure 8 shows the results of rate of absorption of water of REF, BC1, BC2, and BC3, where REF-BC1 and BC2-BC3 are overlaped, respectively. REF and BC1 had the highest rate of absorption of water, which indicated that BC1 had the same water absorption rate as REF and it can be inferred that the BC1 coating behaved like an impregnation, was absorbed by the concrete and did not present resistance to water absorption by capillarity. BC2 and BC3 had the lowest rate of absorption of water, and it can be inferred that the BC2 coating formed a layer with sufficient water absorption rate compared to BC3, so one more layer (BC3) is not necessary to improve that property.

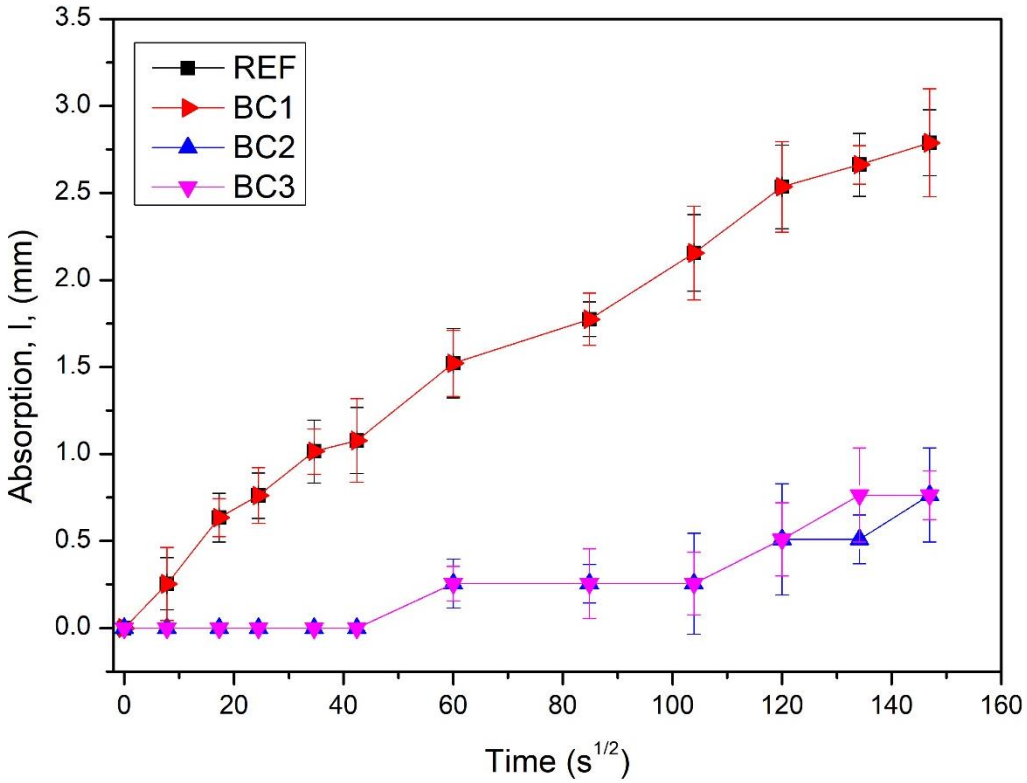

 doi:10.20944/preprints202404.0661.v1

Figure 8. Water absorption rate graph of the uncoated (REF) and coated concrete specimens (BC1, BC2, and BC3).

3.5.2. Permeability of Ion Chloride

Figure 9 presents the charge passed results for REF, BC1, BC2, and BC3. The samples presented average values of charge passed of 7520, 5958, 2030 and 1775 C for REF, BC1, BC2 and BC3, respectively. According to to the classification established by ASTM C1202-19 standard, REF and BC1 have a high permeability (> 4000 C), BC2 has a moderate permeability (2000-4000 C) to low permeability (1000-2000 C), and BC3 has a low permeability. A tendency to decrease the permeability of the samples as the number of coating layers increases is observed; BC3 indicates that it has a greater ability to reduce the movement of chloride ions through concrete, but BC2 also has a similar behavior to BC3, because its permeability is at the lower to moderate limit and very close to the upper limit of low permeability.

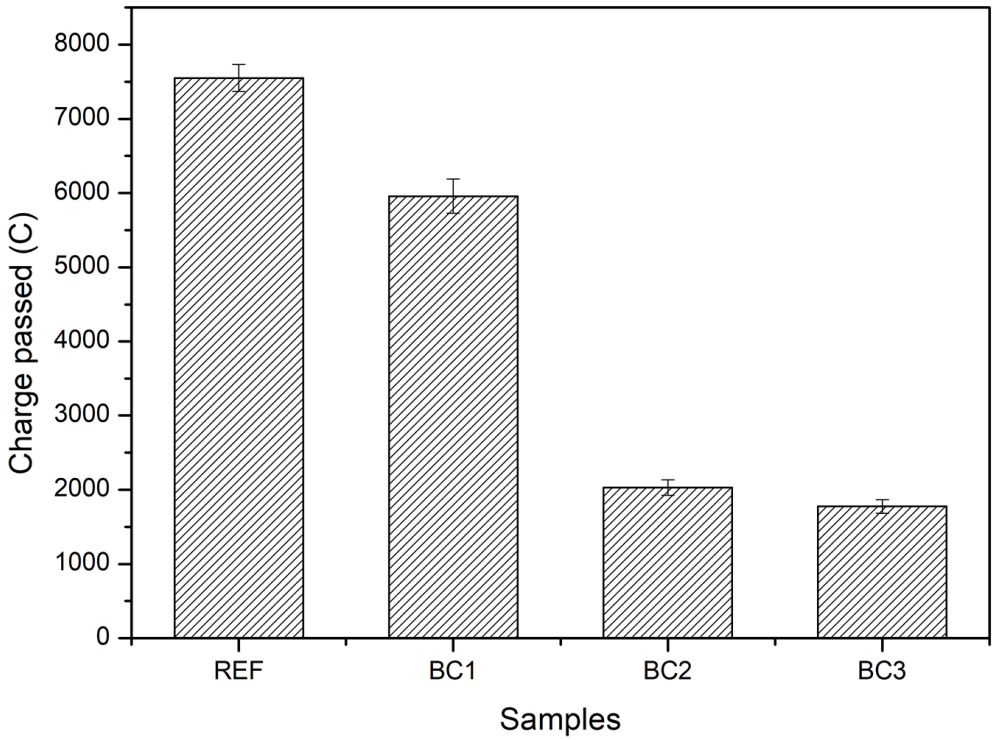

Figure 9. Charge passed to chloride ion in the uncoated (REF) and coated concrete specimens (BC1, BC2, and BC3).

3.5.3. Electrical Resistivity

The Figure 10 presents the average electrical resistivity results for REF, BC1, BC2, and BC3. The average electrical resistivity results were 8.98, 10.24, 23.53, 48.84 kΩ.cm for REF, BC1, BC2 and BC3 respectively. According to CEB-192 standard [58], reinforced concrete with electrical resistivity less than 10 kΩ.cm has a high risk of corrosion. The results showed that the risk of concrete corrosion decreases as the number of PPT coating layers increases. BC2 and BC3 showed a low risk of corrosion.

 doi:10.20944/preprints202404.0661.v1

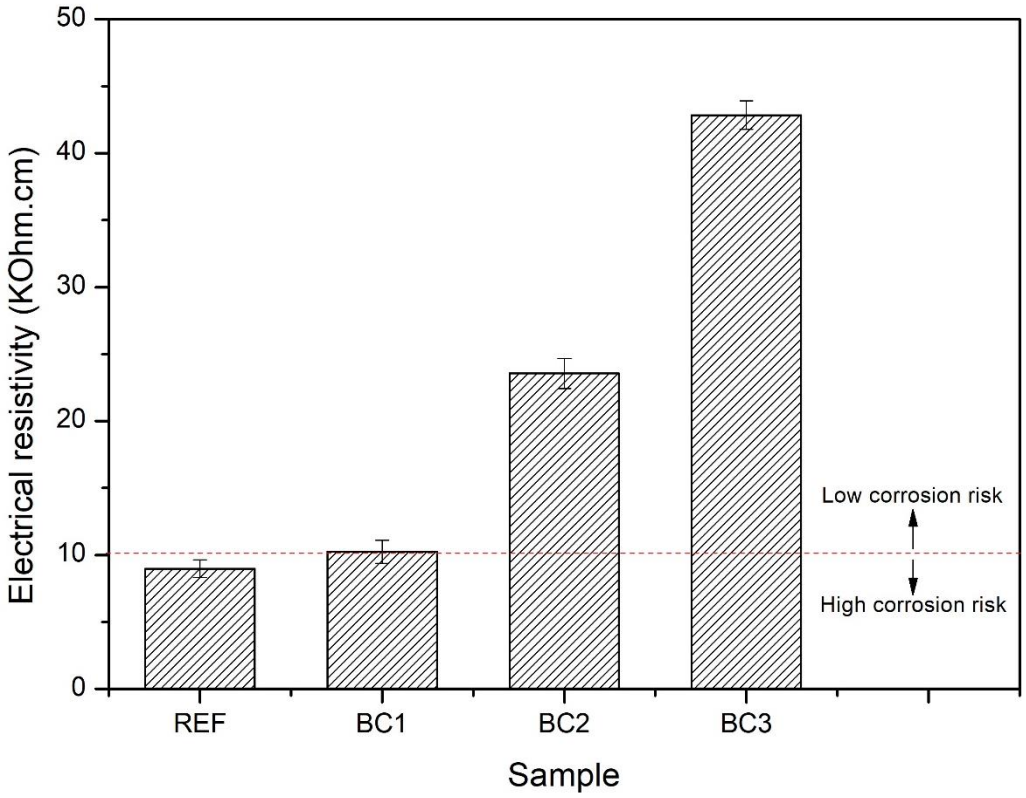

Figure 10. Electrical resistivity of the uncoated (REF) and coated concrete specimens (BC1, BC2, and BC3).

3.5.4. Carbonation Depth

The Figure 11 shows the results of carbonation depth for REF, BC1, BC2 and BC3 at 7, 14, and 28 days of exposure, in which, in the REF and BC1 samples it can be observed that for 7 and 14 days a violet color appears, characteristic of the reaction of phenolphthalein with the non-carbonated zone, and for 28 days this color disappears, which indicates that the sample carbonated; In general, these two samples had a progressive development of carbonation until it was completely produced in a period of 28 days. In samples BC2 and BC3 it can be observed that for 7, 14 and 28 days a violet color appears, which indicates that both samples did not carbonate during that period.

 doi:10.20944/preprints202404.0661.v1

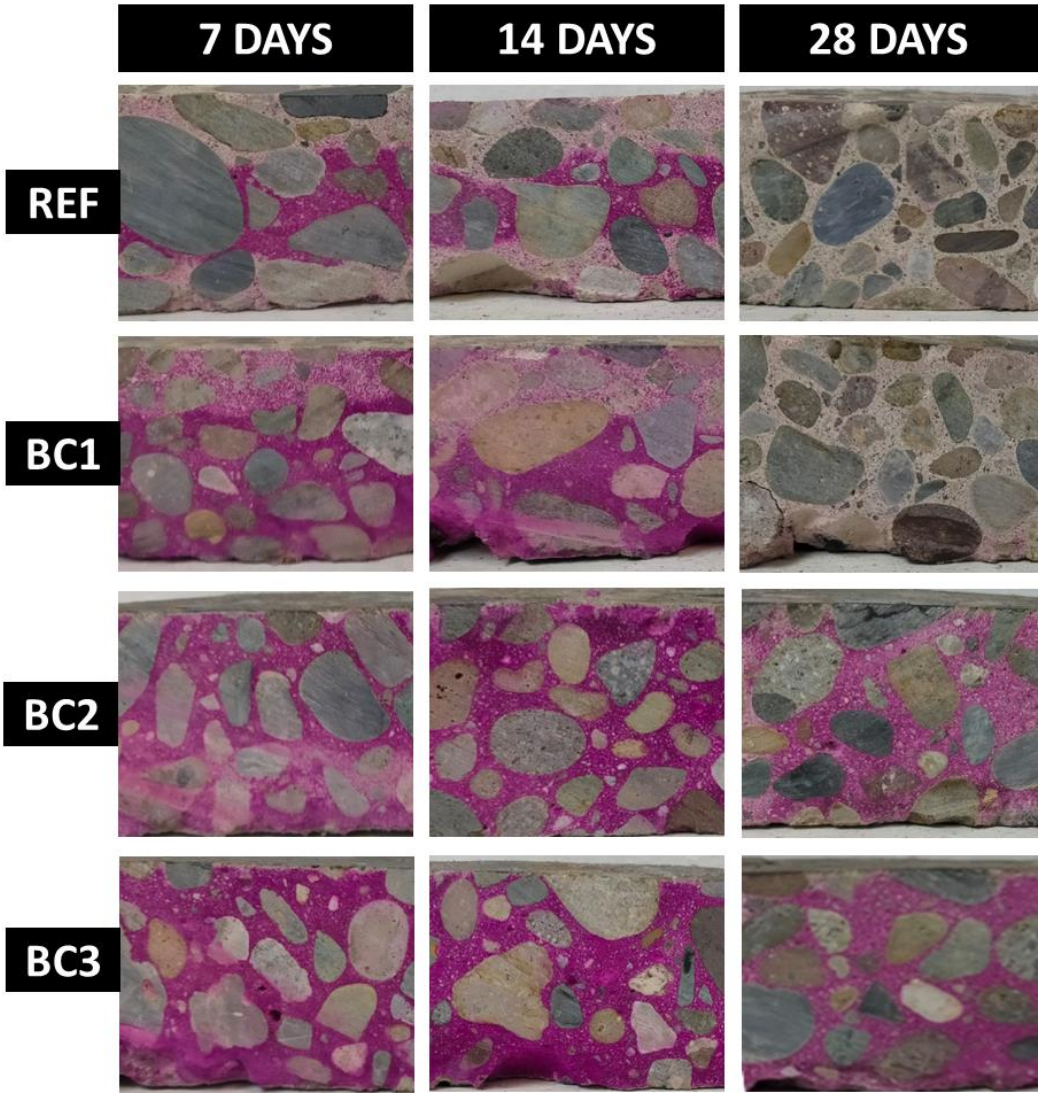

Figure 11. Carbonation depth of uncoated (REF) and coated concrete samples (BC1, BC2 and BC3) at 7, 14 and 28 days of CO_2 exposure.

Table 2 shows the carbonation depth measurements for REF, BC1, BC2, and BC3. The values for REF and BC1 are very similar, which indicate one coating layer did not enough to offer protection to the concrete against CO_2. The measures for BC2 and BC3 are same, these coatings served as a protective barrier against CO_2, this may be due to the chemical composition of the material with which the concrete was coated is similar to that of PET, which is why the material can have the characteristic of being chemically inert, in this case with the accelerated CO_2 environment [59-60].

Table 2. Carbonation depth measurements for uncoated (REF) and coated concrete specimens (BC1, BC2 and BC3) at 7, 14, and 28 days of CO_2 exposure.

Carbonation depth (mm)				
Exposure time/samples	**REF**	**BC1**	**BC2**	**BC3**
7 days	14.97	11.27	0	0
14 days	15.65	15.65	0	0
28 days	25	25	0	0

 doi:10.20944/preprints202404.0661.v1

4. Conclusions

A new brush-applied PPT coating on hydraulic concrete substrate was synthesized by step-growth polymerization of BHPT obtained from recycled PET bottles.

A proposed reaction mechanism for the synthesis of PPT from the glycolysis of PET was established.

The transformation of PET to PPT was achieved, confirmed by FT-IR, because the incorporation of polypropylene groups in the PET molecule was verified by the appearance of CH_3 groups and a significant reduction of OH.

The PPT coating had an hydrophilic behavior, similar to that of PET (contact angle), and optimal adhesion (5B, ASTM D3359-17), similar to resins synthesized from glycolyzed PET products. It had a thermal behavior like PET, with initial main degradation at temperature close (312 °C) to that of PET (348 °C).

The PPT coating based on recycled PET improved the durability of hydraulic concrete, the two-layer coatings had good performance as protection for water absorption and carbonation, however, it was necessary to apply three layers to also protect against the penetration of chloride ions and the risk of corrosion, so the use of three layers of PPT (with an average thickness of 2.50 μm) is recommended to protect the coating in the four properties mentioned.

Author Contributions: All authors contributed to the conceptualization. A. B.-M., C.P. B.-D., R.E. N.-J., F.G. C.-C., J.L. A.-S., and J.M. M.-E. performed the methodology. The authors A. B.-M., C.P. B.-D., J.M. M.-E., J.L. A.-S., and A. H.-M., contributed to formal analysis. J.E. L.-P., B.A. G.-G., J.M. M.-E., and J. F.-V., and J.L. A.-S. worked on written the first draft of the manuscript. All authors commented on previous versions of the manuscript, also, writing-review and editing. J.L. A.-S and A. H.-M. managed the acquisition of materials and resources for the development of the project. and J.L. A.-S was responsible for the administration, supervision and funding adquisition of the project.

Funding: This research was funded by A) The DGIP at the Universidad Autónoma de Sinaloa (UAS) through the PROFAPI2022/PRO_A8_027 Project, B) The Consejo Nacional de Humanidades Ciencia y Tecnología (CONAHCYT) for their support of scholarships No. 924109, C) The Centro de Investigación en Materiales Avanzados, S.C. (CIMAV), for its support in the infrastructure and equipment, for the development of this work.

Data Availability Statement: Not applicable for that section.

Acknowledgments: The authors acknowledge the support of the DGIP of the Universidad Autónoma de Sinaloa (UAS), for the financial support through the PROFAPI2022/PRO_A8_027 Project, to the Consejo Nacional de Humanidades Ciencia y Tecnología (CONAHCYT) for their support of scholarships No. 924109, and to the Centro de Investigación en Materiales Avanzados-Chihuahua (CIMAV) for its support in the infrastructure and equipment, for the development of this work. Additionally, the authors thank CIMAV technicians MSc Karla Campos, PhD Manuel Román and Ing. Roberto Pablo Talamantes, for their important help in the characterizations and UAS students Yamilet Viridiana Moreno Rubio and Adilene Margarita Torres Beltrán, for their important help in the laboratory.

Conflicts of Interest: The authors declare no conflict of interest.

References

1. Trincardi, F.; Francocci, F.; Pellegrini, C.; Ribera d'Alcalà, M.; Sprovieri, M. 13 - The Mediterranean Sea in the Anthropocene. In Oceanography of the Mediterranean Sea, Elsevier, 2023, pp. 501–553. https://doi.org/10.1016/B978-0-12-823692-5.00013-3
2. Benyathiar, P.; Kumar, P.; Carpenter, G.; Brace, J.; Mishra, D.K. Polyethylene Terephthalate (PET) Bottle-to-Bottle Recycling for the Beverage Industry: A Review. *Polymers* **2022,** *14*, 2366. https://doi.org/10.3390/polym14122366
3. Kibria, M.G.; Masuk, N.I.; Safayet, R.; Nguyen, H.Q.; Mourshed, M. Plastic Waste: Challenges and Opportunities to Mitigate Pollution and Effective Management. *Int J Environ Res* **2023,** *17*, 1-37. https://doi.org/10.1007/s41742-023-00507-z
4. Sharifian, S.; Asasian-Kolur, N. Polyethylene terephthalate (PET) waste to carbon materials: Theory, methods and applications. *J. Anal. Appl. Pyrolysis* **2022,** *163*, 105496. https://doi.org/10.1016/j.jaap.2022.105496
5. Jia, Z.; Gao, L.; Qin, L.; Yin, J. Chemical recycling of PET to value-added products. *RSC Sustain.* **2023,** *1*, 2135–2147. https://doi.org/10.1039/d3su00311f

6. Kirshanov, K.; Toms, R.; Aliev, G.; Naumova, A.; Melnikov, P.; Gervald, A. Recent Developments and Perspectives of Recycled Poly(ethylene terephthalate)-Based Membranes: A Review. *Membranes* **2022**, *12*, 1105. https://doi.org/10.3390/membranes12111105
7. Chirayil, C.J.; Mishra, R.K.; Thomas, S. 2 - Materials Recovery, Direct Reuse and Incineration of PET Bottles. In Plastic Design Library, Recycling of Polyethylene Terephthalate Bottles, 1st ed.; Thomas, S.; Rane, A.; Kanny, K.; V.K. Abithia.; Thomas, M.G.; William Andrew Publishing: Oxford, United Kingdom, 2019; pp. 37–60. https://doi.org/10.1016/B978-0-12-811361-5.00003-1
8. Sheel, A.; Pant D. 4 - Chemical Depolymerization of PET Bottles via Glycolysis. In Plastics Design Library, Recycling of Polyethylene Terephthalate Bottles, 1st ed.; Thomas, S.; Rane, A.; Kanny, K.; V.K. Abithia.; Thomas, M.G.; William Andrew Publishing: Oxford, United Kingdom, 2019; pp. 61-84. https://doi.org/10.1016/B978-0-12-811361-5.00004-3
9. Ikladious, N.E.; Asaad, J.N.; Emira, H.S.; Mansour, H.S. Alkyd resins based on hyperbranched polyesters and PET waste for coating applications. *Prog. Org. Coatings* **2017,** *102*, 217–224. https://doi.org/10.1016/j.porgcoat.2016.10.015
10. Bórquez-Mendivil, A.; Hurtado-Macías, A.; Leal-Pérez, J.E.; Flores-Valenzuela, J.; Vargas-Ortíz, R.Á.; Cabrera-Covarrubias, F.G.; Almaral-Sánchez, J.L. Hybrid Coatings of SiO_2–Recycled PET Unsaturated Polyester Resin by Sol-Gel Process. *Polymers* **2022,** *14*, 3280. https://doi.org/10.3390/polym14163280
11. Bal, K.; Ünlü, K.C.; Acar, I.; Güçlü, G. Epoxy-based paints from glycolysis products of postconsumer PET bottles: synthesis, wet paint properties and film properties. *J. Coatings Technol. Res.* **2017,** *14*, 747–753. https://doi.org/10.1007/s11998-016-9895-0
12. Silva, E.; Fedel, M.; Deflorian, F.; Cotting, F.; Lins, V. Properties of Post-Consumer Polyethylene Terephthalate Coating Mechanically Deposited on Mild Steels. *Coatings* **2019,** *9*, 28. https://doi.org/10.3390/coatings9010028
13. Guo, Y.; Xia, X.; Ruan, J.; Wang, Y.; Zhang, J.; LeBlanc, G.A.; An, L. Ignored microplastic sources from plastic bottle recycling. *Sci. Total Environ.* **2022,** *838*, *Part 2*, 156038. https://doi.org/10.1016/j.scitotenv.2022.156038
14. Harusato, A.; Seo, W.; Abo, H.; Nakanishi, Y.; Nishikawa, H.; Itoh, Y. Impact of particulate microplastics generated from polyethylene terephthalate on gut pathology and immune microenvironments. *iScience* **2023,** *26, 4,* 106474. https://doi.org/10.1016/j.isci.2023.106474
15. Yu, J.; Yao, J.; Lin, X.; Li, H.; Lam, J.Y.K.; Leung, C.K.Y.; Sham, I.M.L.; Shih, K. Tensile performance of sustainable Strain-Hardening Cementitious Composites with hybrid PVA and recycled PET fibers. *Cem. Concr. Res.* **2018,** *107*, 110–123. https://doi.org/10.1016/j.cemconres.2018.02.013
16. Chinchillas-Chinchillas, M.J.; Gaxiola A.; Alvarado-Beltrán, C.G.; Orozco-Carmona, V.M.; Pellegrini-Cervantes, M.J.; Rodríguez-Rodríguez, M.; Castro-Beltrán, A. A new application of recycled-PET/PAN composite nanofibers to cement–based materials *J. Clean. Prod.* **2020,** *252*, https://doi.org/10.1016/j.jclepro.2019.119827
17. Tang, R.; Wei, Q.; Zhang, K.; Jiang, S.; Shen, Z.; Zhang, Y.; Chow, C.W.K. Preparation and performance analysis of recycled PET fiber reinforced recycled foamed concrete. *J. Build. Eng.* **2022,** *57*, 104948. https://doi.org/10.1016/j.jobe.2022.104948
18. Noroozi, R.; Shafabakhsh, G.; Kheyroddin, A.; Mohammadzadeh Moghaddam, A. Investigating the effects of recycled PET particles, shredded recycled steel fibers and Metakaolin powder on the properties of RCCP. *Constr. Build. Mater.* **2019,** *224*, 173–187. https://doi.org/10.1016/j.conbuildmat.2019.07.012
19. Gao, Y.; Romero, P.; Zhang, H.; Huang, M.; Lai, F. Unsaturated polyester resin concrete: A review. *Constr. Build. Mater.* **2019,** *228*, 116709. https://doi.org/10.1016/j.conbuildmat.2019.116709
20. Li, C.; Li, J.; Ren, Q.; Zheng, Q.; Jiang, Z. Durability of concrete coupled with life cycle assessment: Review and perspective. *Cem. Concr. Compos.* **2023,** *139*, 105041. https://doi.org/10.1016/j.cemconcomp.2023.105041
21. Rumman, R.; Bari, M.S.; Manzur, T.; Kamal, M.R.; Noor, M.A. A Durable Concrete Mix Design Approach using Combined Aggregate Gradation Bands and Rice Husk Ash Based Blended Cement. *J. Build. Eng.* **2020,** *30*, 101303. https://doi.org/10.1016/j.jobe.2020.101303
22. Merah, A.; Khenfer, M.M.; Korichi, Y. The effect of industrial coating type acrylic and epoxy resins on the durability of concrete subjected to accelerated carbonation *J. Adhes. Sci. Technol.* **2015,** *29*, 2446–2460. https://doi.org/10.1080/01694243.2015.1067004
23. Xia, K.; Gu, Y.; Jiang, L.; Guo, M.; Chen, L.; Hu, F. Carbonation Resistance of Surface Protective Materials Modified with Hybrid NanoSiO_2. *Coatings* **2021,** *11*, 269. https://doi.org/10.3390/coatings11030269
24. Zhang, P.; Li, P.; Fan, H.; Shang, H.; Guo, S.; Zhao, T. Carbonation of Water Repellent-Treated Concrete. *Adv. Mater. Sci. Eng.* **2017,** *2017*, https://doi.org/10.1155/2017/1343947
25. Nashed, Y.L.; Zahran, F.; Youssef, M.A.; Mohamed, M.G.; Mazrouaa, A.M. Performance evaluation of acrylate terpolymer based coating on anti-carbonation. *Pigment Resin Technol.* **2022.** https://doi.org/10.1108/PRT-06-2022-0071

26. Pan, X.; Shi, C.; Zhang, J.; Jia, L.; Chong, L. Effect of inorganic surface treatment on surface hardness and carbonation of cement-based materials. *Cem. Concr. Compos.* **2018,** *90*, 218–224. https://doi.org/10.1016/j.cemconcomp.2018.03.026
27. Lo, T.Y.; Liao, W.; Wong, C.K.; Tang, W. Evaluation of carbonation resistance of paint coated concrete for buildings. *Constr. Build. Mater.* **2016,** *107*, 299–306. https://doi.org/10.1016/j.conbuildmat.2016.01.026
28. Moon, H.Y.; Shin, D.G.; Choi, D.S. Evaluation of the durability of mortar and concrete applied with inorganic coating material and surface treatment system. *Constr. Build. Mater.* **2007,** 21, 362–369. https://doi.org/10.1016/j.conbuildmat.2005.08.012
29. Zheng, W.; Chen, W.G.; Feng, T.; Li, W.Q.; Liu, X.T.; Dong, L.L.; Fu, Y.Q. Enhancing chloride ion penetration resistance into concrete by using graphene oxide reinforced waterborne epoxy coating. *Prog. Org. Coatings* **2020,** *138*, 105389. https://doi.org/10.1016/j.porgcoat.2019.105389
30. Sakr, M.R.; Bassuoni, M.T. Effect of Nano-Based Coatings on Concrete under Aggravated Exposures. *J. Mater. Civ. Eng.* **2020,** *32*, 04020284. https://doi.org/10.1061/(asce)mt.1943-5533.0003349
31. Zhang, P.; Wang, W.; Lv, Y.; Gao, Z.; Dai, S. Effect of Polymer Coatings on the Permeability and Chloride Ion Penetration Resistances of Nano-Particles and Fibers-Modified Cementitious Composites. *Polymers* **2022,** *14*, 3258. https://doi.org/10.3390/polym14163258
32. Medeiros, M.; Helene, P. Efficacy of surface hydrophobic agents in reducing water and chloride ion penetration in concrete. *Mater. Struct. Constr.* **2008,** *41*,59–71. https://doi.org/10.1617/s11527-006-9218-5
33. Bao, J.; Li, S.; Zhang, P.; Xue, S.; Cui, Y.; Zhao, T. Influence of exposure environments and moisture content on water repellency of surface impregnation of cement-based materials. *J. Mater. Res. Technol.* **2020,** *9*, 12115–12125. https://doi.org/10.1016/j.jmrt.2020.08.046
34. Li, J.; Chen, P.; Cai, H.; Xu, Y.; Rasulov, M. Investigation of Silane Impregnation for Protection of Alkali-Activated Slag Mortar. *Adv. Mater. Sci. Eng.* **2021,** *2021*, 9970753. https://doi.org/10.1155/2021/9970753
35. Husni, H.; Nazari, M.R.; Yee, H.M.; Rohim, R.; Yusuff, A.; Mohd Ariff, M.A.; Ahmad, N.N.R.; Leo, C.P.; Junaidi, M.U.M. Superhydrophobic rice husk ash coating on concrete. *Constr. Build. Mater.* **2017,** *144*, 385–391. https://doi.org/10.1016/j.conbuildmat.2017.03.078
36. Carneiro, A.F.B.; Daschevi, P.A.; Langaro, E.A.; Pieralisi, R.; Medeiros, M.H.F. Effectiveness of surface coatings in concrete: chloride penetration and carbonation. *J. Build. Pathol. Rehabil.* **2021,** *6*, 1-8. https://doi.org/10.1007/s41024-020-00098-8
37. ACI PRC-211.1-22: Standard Practice for Selecting Proportions for Normal, Heavyweight, and Mass Concrete. **2022.**
38. ASTM International. ASTM D3359-17: Standard Test Methods for Rating Adhesion by Tape Test. ASTM International **2017**, 06.01, 1-9. https://doi.org/10.1520/D3359-17
39. ASTM International. ASTM C1585-20: Standard Test Method for Measurement of Rate of Absorption of Water by Hydraulic-Cement Concretes. ASTM International **2020.** https://doi.org/10.1520/C1585-20
40. ASTM International. ASTM C1202-19: Standard Test Method for Electrical Indication of Concrete's Ability to Resist Chloride Ion Penetration. ASTM International **2019**. https://doi.org/10.1520/C1202-19
41. CPC-18 Measurement of hardened concrete carbonation depth. *Materials and Structures* **1988,** *21*, 453–455. https://doi.org/10.1007/BF02472327
42. Ravve, A. Principles of Polymer Chemistry, 3rd ed.; Springer New York, 2012; pp. 412-419.
43. Kumar, A.; Gupta, R.K. Fundamentals of Polymer Engineering. Third edition.; CRC Press, 2000; pp. 47-52.
44. Park, S.; Thanakkasaranee, S.; Shin, H.; Lee, Y.; Tak, G.; Seo, J. Pet/bio-based terpolyester blends with high dimensional thermal stability. *Polymers* **2021,** *13*, 1–13. https://doi.org/10.3390/polym13050728
45. Pingale, N.D.; Palekar, V.S.; Shukla, S.R. Glycolisis of Postconsumer Polyehtylene Terephthalate Waste. *J. Appl. Polym. Sci.* **2010,** *115*, 249–254. https://doi.org/10.1002/app.31092
46. Tawfik, M.E.; Elsabee, M.Z. Preparation and Characterization of Polyester Based on bis- (2- hydroxypropyl terephthalate). *J. Polym. Res.* **2002,** *9*, 129–133. https://doi.org/10.1023/A:1021146002662
47. Stuart, B.H. Infrared Spectroscopy: Fundamentals and Applications, 1st ed.; John Wiley & Sons, Ltd, 2004; pp. 71-93.
48. Gall, M.; Freudenthaler, P.J.; Fischer, J.; Lang, R.W. Characterization of Composition and Structure–Property Relationships of Commercial Post-Consumer Polyethylene and Polypropylene Recyclates. *Polymers* **2021,** *13*, 1574. https://doi.org/10.3390/polym13101574
49. Miandad, R.; Reahn, M.; Barakat, M.A..; Aburiazaiza, A.S.; Khan, H.; Ismail, I.M.I.; Dhavamani, J.; Gardy, J.; Hassanpour, A.; Nizami, A-S. Catalytic pyrolysis of plastic waste: Moving toward pyrolysis based biorefineries. *Front. Energy Res.* **2019,** *7*, 1–17. https://doi.org/10.3389/fenrg.2019.00027
50. Chowdhury, T.; Wang, Q. Study on Thermal Degradation Processes of Polyethylene Terephthalate Microplastics Using the Kinetics and Artificial Neural Networks Models. *Processes* **2023,** *11*, 496. https://doi.org/10.3390/pr11020496
51. Ibnu Ali, B.T.; Nareswari, C.; Gunawan, T.; Widiastuti, N.; Kusumawati, Y.; Jaafar, J.; Saputra, H.; Sulistiono, D.O. Utilization of plastic bottle waste of polyethylene terephthalate as a low-cost membrane

 doi:10.20944/preprints202404.0661.v1

and its modifications for gas separation. *J. Ind. Eng. Chem.* **2023,** *127*, 378–389. https://doi.org/10.1016/j.jiec.2023.07.022
52. Chen, Y.; Wang, Z.; Chen, G.; Wang, Q.; Sun, T.; Zhang, M.; Du, Z.; Wu, M.; Guo, S.; Lei, T.; Burra, K.G.; Gupta, A.K. Synergistic effects and products yield analyses based on co-pyrolysis of poplar tree and rape stalks with polyethylene terephthalate and polypropylene. *J. Energy Inst.* **2024,** *112*, 101461. https://doi.org/10.1016/j.joei.2023.101461
53. Ducoli, S.; Federici, S.; Cocca, M.; Gentile, G.; Zendrini, A.; Bergese, P.; Depero, L.E. Characterization of polyethylene terephthalate (PET) and polyamide (PA) true-to-life nanoplastics and their biological interactions. **2024,** *343*, 123150. https://doi.org/10.1016/j.envpol.2023.123150
54. Kim, J.K.; Jeong, Y.S.; Kim, J.W.; Kim, J.S. Two-stage thermochemical conversion of polyethylene terephthalate using steam to produce a clean and H2- and CO-rich syngas. *Energy* **2023,** *276*, 127651. https://doi.org/10.1016/j.energy.2023.127651
55. Benke, A.; Sonnenberg, J.; Oelschlägel, K.; Schneider, M.; Lux, M.; Potthoff, A. Wettability after Artificial and Natural Weathering of Polyethylene Terephthalate. *Environments* **2022,** *9*, 134. https://doi.org/10.3390/environments9110134
56. Caliskan, T.D.; Wei, L.; Luzinov, I. Perfluoropolyether-based oleophobic additives: Influence of molecular weight distribution on wettability of polyethylene terephthalate films. *J. Fluor. Chem.* **2021,** *244*, 109747. https://doi.org/10.1016/j.jfluchem.2021.109747
57. Vesel, A.; Zaplotnik, R.; Primc, G.; Mozetič, M. Evolution of the Surface Wettability of PET Polymer upon Treatment with an Atmospheric-Pressure Plasma Jet. *Polymers* **2020,** *12*, 87. https://doi.org/10.3390/polym12010087
58. Comité Euro International du Béton (1989) CEB Bull 192: diagnosis and assessment of concrete structures—state of the art report, Lausanne
59. Marsh K.; Bugusu, B. Food packaging - Roles, materials, and environmental issues: Scientific status summary. *J. Food Sci.* **2007,** *72*, R39-R55. https://doi.org/10.1111/j.1750-3841.2007.00301.x
60. Nisticò, R. Polyethylene terephthalate (PET) in the packaging industry. *Polym. Test.* **2020,** *90*, 106707. https://doi.org/10.1016/j.polymertesting.2020.106707